Ferroelectricity in the Magnetic *E*-Phase of Orthorhombic Perovskites

Ivan A. Sergienko,[1,2] Cengiz Şen,[3] and Elbio Dagotto[1,2]

[1]*Materials Science and Technology Division, Oak Ridge National Laboratory, Oak Ridge, Tennessee 37831, USA*
[2]*Department of Physics & Astronomy, The University of Tennessee, Knoxville, Tennessee 37996, USA*
[3]*National High Magnetic Field Laboratory and Department of Physics, Florida State University, Tallahassee, Florida 32310, USA*

(Received 20 June 2006; published 30 November 2006)

We show that the symmetry of the spin zigzag chain *E* phase of the orthorhombic perovskite manganites and nickelates allows for the existence of a finite ferroelectric polarization. The proposed microscopic mechanism is independent of spin-orbit coupling. We predict that the polarization induced by the *E*-type magnetic order can potentially be enhanced by up to 2 orders of magnitude with respect to that in the spiral magnetic phases of $TbMnO_3$ and similar multiferroic compounds.

DOI: 10.1103/PhysRevLett.97.227204 PACS numbers: 75.80.+q, 75.50.Ee, 77.80.Fm, 77.84.Dy

Introduction.—The switching of the electric polarization **P** by a magnetic field of a few Tesla discovered in $TbMnO_3$ [1] and $TbMn_2O_5$ [2] has ignited enormous interest in a class of materials that can be termed improper magnetic ferroelectrics (IMF's). While there is no intrinsic ferroelectric (FE) instability in the IMF's, **P** emerges due to its coupling to the primary magnetic order parameter. Hence, the FE phase transition coincides with the corresponding magnetic transition, and **P** is very sensitive to magnetic field-induced changes of the magnetic state [1–9]. Symmetry imposes rather strict conditions on the possible magnetic order parameters—the magnetic structure must have low enough symmetry in order for the system to form a polar axis. As a consequence, the IMF's often have complicated noncollinear structures, including spiral and incommensurate [6–13], while the IMF phases with collinear magnetism are rare [14,15]. Noncollinear magnetic structures are stabilized due to either competing interactions (frustration) or anisotropies generated by spin-orbit coupling, which leads to reduced transition temperatures and weaker order parameters. The magnitude of P ($\approx 0.1\ \mu C/cm^2$) is also affected by its weak coupling to magnetism. In turn, collinear IMF's may prove more promising for future applications as they are less prone to the obstacles mentioned above.

In our present Letter, we turn our attention to the collinear *E*-type magnetic phase that has been observed in perovskite manganites [16,17] and nickelates [18–21]. First, we show that this is a previously overlooked example of an IMF. Second, in contrast to the most extensively theoretically studied case of spiral magnetism [22–24], the mechanism responsible for ferroelectricity in the magnetically ordered phase does not rely on the presence of anisotropic Dzyaloshinskii-Moriya interaction. In our case, **P** appears due to a gain in the band energy of the e_g electrons in the double-exchange model. We estimate that P can be potentially larger than that in the spiral magnets by up to 2 orders of magnitude, thus paving a way for IMF's to reach the values of P common for other multiferroic systems with better ferroelectric properties [25,26].

In the perovskite manganite family $RMnO_3$ (space group *Pbnm*), the *E*-phase was first reported for R = Ho as a result of magnetic structure refinement by neutron diffraction [16]. The magnetic unit cell of the *E*-phase, forming at low temperature below $T_L = 26$–29.6 K [16,27], is shown in Fig. 1(a). The Mn atoms with parallel spins form zigzag chains in the *ab*-plane, with the chain link equal to the nearest-neighbor Mn-Mn distance. The neighboring zigzag chains in the *b*-direction have antiparallel spins. Figs. 1(b) and 1(c) show that the equal-spin *E*-phase structure can be obtained from the simple sine-wave structure by locking-in its modulation vector $k_b = \frac{1}{2}$ and fine-tuning its phase. The *ab*-planes are stacked antiferromagnetically $(+-+-)$ along the *c*-direction. Interestingly, Lorenz *et al.* [27] reported on a large magnetic field dependence of the dielectric constant below T_L, which may be an indication of the multiferroic state.

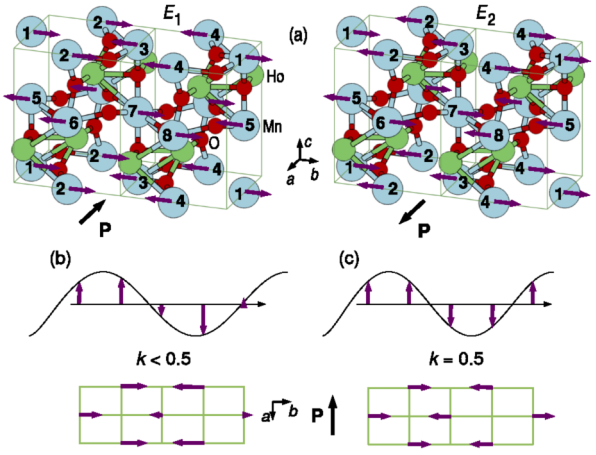

FIG. 1 (color online). (a) Magnetic unit cells of the two *E*-phase domains in $HoMnO_3$ corresponding to the (E_1, 0, $-P_a$) and (0, E_2, P_a) solutions of (2). The arrows on the Mn atoms denote the directions of their spins. The FE displacements are not shown, but the direction of **P** is indicated. (b) The simple sine-wave magnetic structure of $HoMnO_3$ for $T_L < T < T_N = 42.2$–47.5 K [16]. (c) The *E*-phase magnetic structure below T_L.

Landau theory.—Independently of the microscopic mechanism, the possibility of a FE state in magnets can be examined by considering the symmetry allowed terms in the Landau potential [6,11,24,28,29]. We define the symmetric coordinates corresponding to the E-phase as

$$\begin{aligned}\mathbf{E}_1 &= \mathbf{S}_1 + \mathbf{S}_2 - \mathbf{S}_3 - \mathbf{S}_4 - \mathbf{S}_5 - \mathbf{S}_6 + \mathbf{S}_7 + \mathbf{S}_8,\\ \mathbf{E}_2 &= \mathbf{S}_1 - \mathbf{S}_2 - \mathbf{S}_3 + \mathbf{S}_4 - \mathbf{S}_5 + \mathbf{S}_6 + \mathbf{S}_7 - \mathbf{S}_8,\end{aligned} \quad (1)$$

where $\mathbf{S}_i$ is the spin of the ith Mn atom in the magnetic unit cell, as shown in Fig. 1(a). Since the Mn spins in $HoMnO_3$ point along the b-axis [16], below we consider only the b-components of $\mathbf{E}_{1,2}$ denoted by $E_{1,2}$. However, the expression for the Landau potential derived below is valid for any component of $\mathbf{E}_{1,2}$. E_1 and E_2 span an irreducible representation of the space group $Pbnm$ corresponding to $\mathbf{k} = (0\,\frac{1}{2}\,0)$. The properties of this representation are summarized in Table I. Taking into account that $\mathbf{P}$ transforms as a polar vector, we obtain the following form of the Landau potential corresponding to the E-phase,

$$\begin{aligned}F = {} & a(E_1^2 + E_2^2) + b_1(E_1^2 + E_2^2)^2 + b_2 E_1^2 E_2^2 \\ & + c(E_1^2 - E_2^2)P_a + d(E_1^2 - E_2^2)E_1 E_2 P_b + \frac{1}{2\chi}\mathbf{P}^2,\end{aligned} \quad (2)$$

where χ is the dielectric susceptibility of the paraelectric phase, and the other coefficients are phenomenological parameters. Minimizing F with respect to $\mathbf{P}$, we obtain $P_a = -c\chi(E_1^2 - E_2^2)$, $P_b = -d\chi(E_1^2 - E_2^2)E_1E_2$, and $P_c = 0$. Therefore, each of the four domains of the E-phase [$(\pm E_1, 0)$ and $(0, \pm E_2)$] is IMF with the polarization along the a-axis and different signs of P_a for E_1 and E_2. We also notice that the b-axis component of $\mathbf{P}$ can be locally present within the domain walls where E_1 and E_2 coexist [30].

The E-type phase in the nickelates also consists of spin zigzag chains that have a different direction in the ab-plane and a different stacking along the c-axis ($+\,+\,-\,-$) [18–21]. The corresponding modulation vector is $\mathbf{k} = (\frac{1}{2}\,0\,\frac{1}{2})$. The Landau theory analysis leads to results similar to the manganite case. For nickelates, the symmetric coordinates E_1 and E_2 (not given here) are written in terms of 16 Ni spins of the magnetic unit cell which is 4 times the crystallographic unit cell. It leads to a Landau potential similar to (2) with P_a replaced by P_b in the fourth term and $d = 0$.

TABLE I. Matrices of the generators of space group $Pbnm$ in the irreducible representation spanned by E_1, E_2. The space group elements are denoted $(r|hkl)$, where r is the identity operation 1, twofold rotation $2_{a,c}$, inversion I, or time reversal $1'$ followed by the translation $\tau = h\mathbf{a} + k\mathbf{b} + l\mathbf{c}$.

	$(2_a\|\frac{1}{2}\,\frac{1}{2}0)$	$(2_c\|00\,\frac{1}{2})$, $(I\|000)$	$(1\|010)$, $(1'\|000)$
E_1	$-1\ 0$	$0\ 1$	$-1\ 0$
E_2	$0\ 1$	$1\ 0$	$0\ -1$

Thus, $\mathbf{P}$ in the E-phase of nickelates is parallel to the b-axis.

Microscopic model.—To understand microscopically the possible mechanism of ferroelectricity in the E-phase, we use Monte Carlo (MC) simulations to study the ground state properties of the following Hamiltonian for manganites based on the orbitally degenerate double-exchange model [31–33] with one e_g-electron per Mn^{3+} ion,

$$\begin{aligned}H = {} & -\sum_{\mathbf{ia}\alpha\beta} C_{\mathbf{i},\mathbf{i}+\mathbf{a}} t^{\mathbf{ia}}_{\alpha\beta} d^\dagger_{\mathbf{i}\alpha} d_{\mathbf{i}+\mathbf{a}\beta} + J_{\mathrm{AF}} \sum_{\mathbf{ia}} \mathbf{S}_{\mathbf{i}} \cdot \mathbf{S}_{\mathbf{i}+\mathbf{a}} \\ & + \lambda \sum_i (Q_{1\mathbf{i}}\rho_{\mathbf{i}} + Q_{2\mathbf{i}}\tau_{x\mathbf{i}} + Q_{3\mathbf{i}}\tau_{z\mathbf{i}}) + \frac{1}{2}\sum_{\mathbf{i}m} \kappa_m Q^2_{m\mathbf{i}},\end{aligned} \quad (3)$$

where $d^\dagger_{\mathbf{i}\alpha}$ is the creation operator for the e_g electron on orbital $\alpha = x^2 - y^2(a)$, $3z^2 - r^2(b)$; $\mathbf{a} = \mathbf{x}, \mathbf{y}$ is the direction of the link connecting the two nearest-neighbor Mn sites; and $\mathbf{S_i}$ is the classical unit spin, given by the polar angle $\theta_{\mathbf{i}}$ and azimuthal angle $\phi_{\mathbf{i}}$, representing the electrons occupying the t_{2g} orbitals on the $\mathbf{i}$-th Mn site. The t_{2g} spins interact directly through the antiferromagnetic superexchange $J_{\mathrm{AF}} > 0$. $C_{\mathbf{i},\mathbf{j}} = \cos\frac{\theta_{\mathbf{i}}}{2}\cos\frac{\theta_{\mathbf{j}}}{2} + \sin\frac{\theta_{\mathbf{i}}}{2}\sin\frac{\theta_{\mathbf{j}}}{2}e^{-i(\phi_{\mathbf{i}}-\phi_{\mathbf{j}})}$ is the double-exchange factor arising due to the large Hund's coupling that projects out the e_g electrons with spin antiparallel to $\mathbf{S}_i$. $Q_{m\mathbf{i}}$ represent the classical adiabatic phonon modes, with stiffnesses κ_m, due to the displacements of the ligand oxygen ions surrounding the $\mathbf{i}$-th Mn site. The phonon stiffnesses were chosen as follows—for the Jahn-Teller modes: $\kappa_1 = 2.0$, $\kappa_2 = \kappa_3 = 1.0$; for the FE mode: $\kappa_{\mathrm{FE}} = 8.0$; and for the rest of the modes: $\kappa = 10.0$. Except for the Jahn-Teller modes [31,32], this choice is driven only by the efficiency of the MC simulations, and it does not reflect the actual frequencies of the phonon modes, which are presently unknown. We illustrate below how P can be obtained in physical units. The third term in Eq. (3) is the Jahn-Teller coupling with constant λ and the e_g-orbital operators $\rho_{\mathbf{i}} = d^\dagger_{\mathbf{i}a}d_{\mathbf{i}a} + d^\dagger_{\mathbf{i}b}d_{\mathbf{i}b}$, $\tau_{x\mathbf{i}} = d^\dagger_{\mathbf{i}a}d_{\mathbf{i}b} + d^\dagger_{\mathbf{i}b}d_{\mathbf{i}a}$, and $\tau_{z\mathbf{i}} = d^\dagger_{\mathbf{i}a}d_{\mathbf{i}a} - d^\dagger_{\mathbf{i}b}d_{\mathbf{i}b}$.

Our improvements over previous approaches to this model are the following. First, we explicitly consider the dependence of the hoping parameters $t^{\mathbf{ia}}_{\alpha\beta}$ on the angle of the Mn-O-Mn bond $\varphi_{\mathbf{ia}}$. Taking into account only the largest Mn-O σ-bond contribution, we find [34] $t^{\mathbf{x}}_{aa} = t^{\mathbf{y}}_{aa} = -t\cos^3\varphi$, $t^{\mathbf{x}}_{bb} = t^{\mathbf{y}}_{bb} = -t\cos\varphi/3$, $t^{\mathbf{x}}_{ab} = t^{\mathbf{x}}_{ba} = -t^{\mathbf{y}}_{ab} = -t^{\mathbf{y}}_{ba} = -t\cos^2\varphi/\sqrt{3}$, where $t = \frac{3}{4}(pd\sigma)^2$ is taken as the energy unit hereafter. We neglect the φ dependence of J_{AF} since it has a smaller energy scale than t. Second, $Q_{m\mathbf{i}}$'s are defined such that the elastic energy term in (3) is minimal for $\varphi_{\mathbf{ia}} \equiv \varphi_0 < 180°$. This allows us to model the initial structural buckling ($GdFeO_3$-type) distortion present in the orthorhombic perovskites [35]. In particular, the buckling mode is defined in two dimensions as $Q_{\mathrm{buckle},\mathbf{i}} = y_{\mathbf{i}1} - y_{\mathbf{i}2} - x_{\mathbf{i}3} + x_{\mathbf{i}4} - (-1)^{i_x+i_y}4u_0$, where $x_{\mathbf{i}k}$, $y_{\mathbf{i}k}$ are the displacements of the oxygen atoms from their ideal position in the 180° Mn-O-Mn

bond, $u_0 = a_0 \cot\frac{\varphi_0}{2}$, and a_0 is the Mn-O distance in the 180° Mn-O-Mn bond [see Fig. 2(a)]. Since the buckling distortion in the considered perovskites is present at temperatures well above the magnetic transitions, we consider φ_0 as a fixed parameter of the model. For $HoMnO_3$, φ_0 is close to 144° [35]. As shown below, this distortion plays a crucial role in generating ferroelectricity in the E-phase. Introducing $\varphi_0 < 180°$ effectively reduces the symmetry of the Hamiltonian (3) although it is still invariant with respect to the inversion symmetry centers located at the every Mn site. The FE polarization emerges only due to the spontaneous symmetry breaking caused by the E-phase magnetic order.

Monte Carlo results.—Many results of the model (3) regarding magnetic and orbital order, without the modifications mentioned above, are reported in Ref. [32]. Our present treatment essentially confirms those results. The ground state phase diagram in two dimensions contains the ferromagnetic phase, E-phase, and the Neél-like G-phase. Here we focus our attention on the new results directly related to the ferroelectricity of the E-phase. A typical low-temperature E-phase MC snapshot is shown in Fig. 2(b). In accordance with the absence of spin-orbit interaction in Hamiltonian (3), it is invariant with respect to collective spin rotations; therefore, the preferred spin direction is chosen randomly in our MC simulations. However, the ferromagnetic zigzag chains are clearly established in the ground state. As is seen from the snapshot, the double-exchange physics plays a crucial role in the formation of the FE state. Because of the factor $C_{\mathbf{i},\mathbf{i}+\mathbf{a}}$, the electron hopping is prohibited between Mn atoms with opposite t_{2g} spins. Hence, the displacement of the corresponding oxygen atom perpendicular to the Mn-Mn bond (these displacements are not Jahn-Teller active) is only due to the elastic energy, which favors the bond angle φ_0. On the contrary, hopping is allowed along the ferromagnetic zigzag chains [36]. Since hopping energy is minimal for the 180° bond, the competition between the hopping and elastic energies generally results in a bond angle φ, such that $\varphi_0 < \varphi < 180°$ [see Fig. 2(c)]. Since φ only depends on the nature of the bond (ferromagnetic vs antiferromagnetic), the direction of the oxygen displacements is the same in all zigzag chains, even though neighboring chains have opposite spin. This leads to the overall coherent displacement of the center of mass of the O atoms with respect to the Mn sublattice, similarly as proposed in Ref. [15] for the field-induced phase of $TbMnO_3$. It is easy to see from Fig. 2(b) and 2(c) that the resulting FE polarization points along the diagonal connecting the next-nearest-neighboring Mn atoms, i. e., the a-axis in the orthorhombic setting, are in perfect agreement with Landau theory.

The value of P.—Figure 2(d) shows the calculated absolute value of the polarization $P_{\rm calc}$, defined as the oxygen displacement per one "unit cell" containing one Mn and two O atoms averaged over MC steps, plotted versus φ_0 for different values of $J_{\rm AF}$. P vanishes for $\varphi_0 = 180°$ for all values of $J_{\rm AF}$. In this case, both the hopping and elastic energies are optimal when $\varphi = \varphi_0 = 180°$, the same for ferromagnetic and antiferromagnetic bonds. To demonstrate that this is also consistent with the symmetry arguments of Landau theory, we note that the symmetry of the lattice with 180° bonds is higher than that with $\varphi_0 < 180°$. Particularly, additional inversion centers are located at the O sites if $\varphi_0 = 180°$. While the E-type magnetic structure breaks inversion symmetry for centers located at the Mn sites, it is invariant with respect to the O-site centers, and thus the magnetic phase transition cannot induce FE order. In terms of the Landau potential (2), the coefficients c and d must be zero in this case.

The MC calculated value of the polarization $P_{\rm calc}$ for $\varphi_0 \approx 145°$ corresponding to $HoMnO_3$ reaches 0.08. It can be shown from the model (3) that the FE displacements scale as $t/\kappa_{\rm FE} a_0$. In the simulations, we set $t = 1$ and $a_0 = 1$, and the polarization in the physical units, in the point charge approximation, is given by $P = \frac{12 e t \kappa_{\rm FE}}{\kappa'_{\rm FE} a_0 V_0} P_{\rm calc}$, where e is the elementary charge, $\kappa'_{\rm FE}$ is the FE phonon stiffnesses in the physical units, and V_0 is the unit cell volume. Using $a_0 = 2.35$ Å, $V_0 = 226$ Å^3 [16], $t = 0.1$–0.5 eV [31], $\kappa'_{\rm FE} = 1$–5 eV/Å^2 [23], we obtain a range of values for

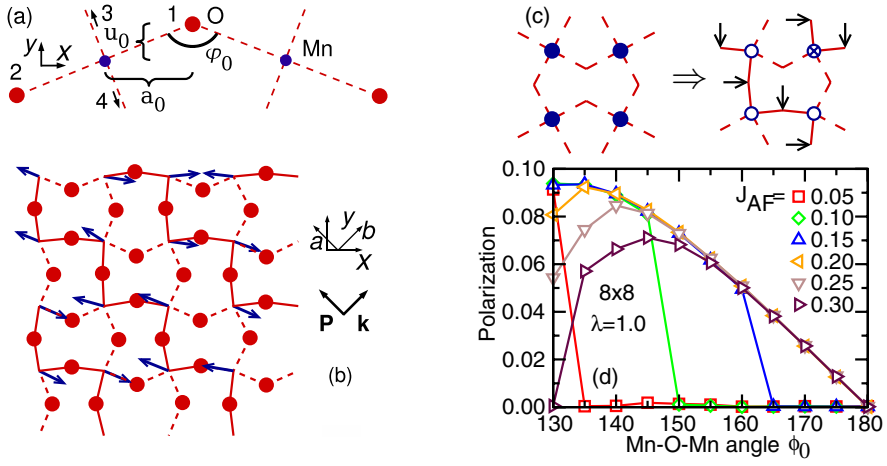

FIG. 2 (color online). (a) The starting configuration of a Mn-O-Mn bond. Numbers 1–4 enumerate the O atoms surrounding one Mn. (b) An MC snapshot of the IMF E-phase at $T = 0.01$. The ferromagnetic zigzag chain links are shown as solid lines. The displacements of the oxygen atoms are exaggerated. (c) Left. The local arrangement of the Mn-O bonds with disordered Mn spins (full circles). Right. Oxygen displacements (arrows) within the chains of opposite Mn spins (open and crossed circles) in the E-phase (see also Refs. [3,15]). (d) MC results for the polarization at $T = 0.01$ for different values of $J_{\rm AF}$.

P between 0.5 and 12 $\mu C/cm^2$, substantially larger than the P observed in helical IMF's. We can also estimate P from the known experimental results for $TbMnO_3$. Its crystal structure is modulated in the collinear sine-wave phase with wave vector $k_L = 2k_M$, where $k_M = 0.29$ is the magnetic wave vector. The displacement of the O atom n in a Mn-O chain running along the x- or y-direction [see Fig. 2(b)] is given by $\delta\mathbf{r}_n = \delta\mathbf{r}_0(-1)^n\{\cos\pi k_M + \cos[(2n+1)\pi k_M + 2\alpha]\}$, for the magnetic structure defined by $S_a = S_c = 0$, $S_b = S_b^0\cos(nk_M + \alpha)$ [23]. If $k_M \neq 1/2$, then $\sum_n \delta r_n^a = 0$ and the state is paraelectric. The E-phase corresponds to $k_M = 1/2$, $\alpha = 3\pi/4$, and hence $\delta\mathbf{r}_n \equiv \delta\mathbf{r}_0$ represents a coherent displacement within one chain. While the b and c components of $\delta\mathbf{r}_0$ have different signs in different chains, δr_0^a's are the same. Considering the $TbMnO_3$ value $\delta r_0 = 10^{-2}$ Å [37] as an estimate for δr_0^a in $HoMnO_3$, we obtain $P \approx 2\ \mu C/cm^2$ consistent with the calculated values.

Summary.—We argue that the symmetry of the spin zigzag chain magnetic E-phase in orthorhombic perovskites with buckling distortion of the oxygen octahedra allows the formation of a polar axis along the a-axis. The microscopic mechanism of ferroelectricity is independent of spin-orbit coupling, and P can potentially be up to 2 orders of magnitude higher than that in the helical IMF's. Note that the ideas described here are general, and the E-phase provides just one example. In fact, the mechanism is similar to the recently proposed explanation for the ferroelectricity found in $TbMnO_3$ at high fields [15], and our effort provides a firm theoretical basis for that interesting scenario. As to the E-phase nickelates, the microscopic model considered here is not applied to them directly [38]. However, we expect that the same interplay between the optimization of the electron hopping and the elastic energy in the presence of the buckling distortion will lead to ferroelectricity.

We thank M. Angst, D. Argyriou, T. Egami, D. Mandrus, and D. Singh for inspiring discussions, as well as T. Kimura and B. Lorenz for providing us with their unpublished results. Research at ORNL is sponsored by the Division of Materials Sciences and Engineering, Office of Basic Energy Sciences, U.S. Department of Energy, under Contract No. DE-AC05-00OR22725 with ORNL, managed and operated by UT-Battelle, LLC. This work is also supported in part by NSF No. DMR-0443144 and NSF No. DMR-0072998. We have used the SPF software developed at ORNL (http://scicompforge.org/spf).

Note added.—Following our prediction, B. Lorenz *et al.* [39] reported on experimental evidence of ferroelectricity in perovskite $HoMnO_3$ and $YMnO_3$. For the latter, the E-phase was proposed in Ref. [17].

[1] T. Kimura *et al.*, Nature (London) **426**, 55 (2003).
[2] N. Hur *et al.*, Nature (London) **429**, 392 (2004).
[3] T. Goto *et al.*, Phys. Rev. Lett. **92**, 257201 (2004).
[4] T. Kimura, G. Lawes, and A. P. Ramirez, Phys. Rev. Lett. **94**, 137201 (2005).
[5] T. Kimura *et al.*, Phys. Rev. B **71**, 224425 (2005).
[6] G. Lawes *et al.*, Phys. Rev. Lett. **95**, 087205 (2005).
[7] L. C. Chapon *et al.*, Phys. Rev. Lett. **96**, 097601 (2006).
[8] T. Kimura, J. C. Lashley, and A. P. Ramirez, Phys. Rev. B **73**, 220401(R) (2006).
[9] Y. Yamasaki *et al.*, Phys. Rev. Lett. **96**, 207204 (2006).
[10] G. R. Blake *et al.*, Phys. Rev. B **71**, 214402 (2005).
[11] M. Kenzelmann *et al.*, Phys. Rev. Lett. **95**, 087206 (2005).
[12] T. Arima *et al.*, Phys. Rev. Lett. **96**, 097202 (2006).
[13] K. Taniguchi *et al.*, Phys. Rev. Lett. **97**, 097203 (2006).
[14] L. C. Chapon *et al.*, Phys. Rev. Lett. **93**, 177402 (2004).
[15] N. Aliouane *et al.*, Phys. Rev. B **73**, 020102(R) (2006).
[16] A. Muñoz, *et al.*, Inorg. Chem. **40**, 1020 (2001).
[17] J.-S. Zhou and J. B. Goodenough, Phys. Rev. Lett. **96**, 247202 (2006).
[18] J. L. García-Muñoz, J. Rodríguez-Carvajal, and P. Lacorre, Phys. Rev. B **50**, 978 (1994).
[19] J. A. Alonso *et al.*, Phys. Rev. Lett. **82**, 3871 (1999).
[20] M. T. Fernández-Díaz *et al.*, Phys. Rev. B **64**, 144417 (2001).
[21] J.-S. Zhou, J. B. Goodenough, and B. Dabrowski, Phys. Rev. Lett. **95**, 127204 (2005).
[22] H. Katsura, N. Nagaosa, and A. V. Balatsky, Phys. Rev. Lett. **95**, 057205 (2005).
[23] I. A. Sergienko and E. Dagotto, Phys. Rev. B **73**, 094434 (2006).
[24] M. Mostovoy, Phys. Rev. Lett. **96**, 067601 (2006).
[25] M. Fiebig, J. Phys. D: Appl. Phys. **38**, R123 (2005).
[26] C. Ederer and N. A. Spaldin, Curr. Opin. Solid State Mater. Sci. **9**, 128 (2005).
[27] B. Lorenz, Y. Q. Wang, Y. Y. Sun, and C. W. Chu, Phys. Rev. B **70**, 212412 (2004).
[28] S. Goshen, D. Mukamel, H. Shaked, and S. Shtrikman, Phys. Rev. B **2**, 4679 (1970).
[29] A. B. Harris, T. Yildirim, A. Aharony, and O. Entin-Wohlman, Phys. Rev. B **73**, 184433 (2006).
[30] Although the E-phase is a special case of the simple sine-wave structure, the continuum theory considered in Ref. [24], which predicts $\mathbf{P} = 0$, is not applicable to modulation vectors at the edge of the Brillouin zone.
[31] E. Dagotto, T. Hotta, and A. Moreo, Phys. Rep. **344**, 1 (2001).
[32] T. Hotta *et al.*, Phys. Rev. Lett. **90**, 247203 (2003).
[33] D. V. Efremov, J. van den Brink, and D. I. Khomskii, Nat. Mater. **3**, 853(2004).
[34] J. C. Slater and G. F. Koster, Phys. Rev. **94**, 1498 (1954).
[35] T. Kimura *et al.*, Phys. Rev. B **68**, 060403(R) (2003).
[36] Although virtual hopping is allowed along the zigzag chains, the E-phase is a band insulator [32].
[37] T. Kimura (private communication).
[38] T. Hotta and E. Dagotto, Phys. Rev. Lett. **92**, 227201 (2004).
[39] B. Lorenz, Y. Q. Wang, and C. W. Chu, cond-mat/0608195.